

Start-up times in viscoelastic channel and pipe flows

A.I.P. Miranda¹ and P.J. Oliveira^{2,*}

¹*Departamento de Matemática,*

²*Departamento de Engenharia Electromecânica, Unidade de Materiais Têxteis e Papeleiros,
Universidade da Beira Interior, 6200-001 Covilhã, Portugal,*

(Received November 2, 2009; final version received January 27, January 27, 2010)

Abstract

Start-up times in viscoelastic channel and pipe flows generated by the sudden imposition of a pressure gradient are here determined by a mixed analytical/numerical procedure. The rheological models considered are the upper convected Maxwell and the Oldroyd-B equations. With these models the flow evolves asymptotically to the steady state solution after a transient regime presenting strong oscillations of the velocity fields, hence implying a special procedure for the calculation of the start-up time. This time interval required for establishment of steady flow tends to increase significantly with elasticity, at a constant rate of increase for the UCM model, but the increase becoming less than linear for the Oldroyd-B model. No wiggles or artificial oscillations were observed for the variation of the start-up times with the elasticity number.

Keywords : start-up flow, channel or pipe flow, transient viscoelastic flow, Oldroyd-B, UCM

1. Introduction

Start-up flow occurs when a constant pressure gradient is suddenly applied to a liquid initially at rest in either a long planar channel or a long circular cross-section pipe. For a Newtonian liquid the analytical solution of this problem was obtained by Bromwich (1930) for the 2D case and by Szymansky (1932) for the axi-symmetric case; the velocity grows monotonically with time until the parabolic velocity profile is obtained asymptotically for large times. If the start-up time (t_s) is defined when the centreline velocity is within a 1% difference from its steady-state value, then the analytical solutions readily give for channel flow $t_s = 1.88 \rho H^2 / \mu$, where H is the half channel width, and for pipe flow $t_s = 0.81 \rho R^2 / \mu$, where R is the pipe radius; ρ and μ are the fluid density and viscosity. Under non-dimensional form, after scaling time with a diffusion time scale, the start-up times for Newtonian fluids are thus $t_s = 1.88$ (channel) or $t_s = 0.81$ (pipe). For viscoelastic liquids obeying either the upper-convected Maxwell (UCM) or the Oldroyd-B constitutive equations (Oldroyd, 1950) things are more complicated, although the transient solution is known (Waters and King, 1970; 1971) and the final steady profile is still parabolic in shape due to the constant shear viscosity of these model fluids. In the present work we intend to obtain by a mixed analytical/ numerical procedure the evolution of the start-up times as a function of

elasticity number and retardation ratio for those rheological models. It will be shown that, due to the oscillating nature of these flows, the definition and calculation of start-up times will require a special procedure in order to filter out those oscillations. Start-up times obtained in this manner for the UCM model will present an initial decreasing tendency with elasticity, followed by an almost linear increase for elasticity numbers (defined below, see Eq. 14) greater than about 0.3 ($t_s: 11.7E$ channel; $t_s: 13.2E$ pipe). For the Oldroyd-B model the rate of growth of the start-up time is less than linear; for example, at a retardation ratio of $\beta = 0.1$, we found $t_s: E^{0.8}$ for channel flow, although a linear fractional variation suggested by the exact solution $t_s: c_1 E / (1 + c_2 \beta E)$ gives an even better fit.

Start-up flows of non-Newtonian viscoelastic fluids (Bird *et al.* 1987) in channels and pipes are particularly relevant for the verification of numerical methods for the calculation of transient flows (Duarte *et al.*, 2008; Park and Kwon, 2009) since, as mentioned above, analytical solutions are available for UCM and Oldroyd-B constitutive models. Waters and King (1970, 1971) were the first to derive those theoretical solutions using a Laplace transform approach and later Rahaman and Ramkissoon (1995) for the UCM model and Woods (2001) for the Oldroyd-B obtained the same solution for start-up of pipe flow using different methods. As an extension, the 3D problem of start-up of the Oldroyd-B fluid in a rectangular cross-section duct was addressed by Akyildiz and Jones (1993) who followed a route similar to Waters and King (1970). None of these authors considered the variation of the start-up

*Corresponding author: pipo@ubi.pt
© 2010 by The Korean Society of Rheology

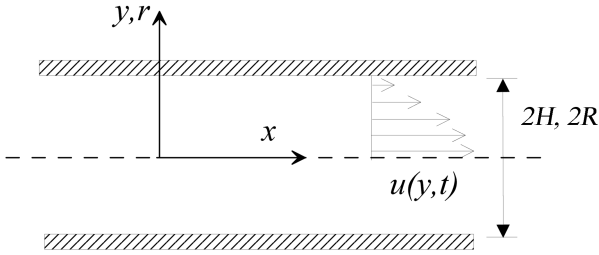


Fig. 1. Sketch of the flow geometry.

time with elasticity. Those transient solutions evolve in time until the same steady state solution valid for Newtonian flows is attained. The time taken for the variable regime to reach conditions close to steady state depends strongly on the elasticity of the fluid. Waters and King (1971) in the pipe flow paper calculated a few start-up times for a limited range of elasticity ($E=0.3, 0.4, 0.5$; $\beta=0.04-0.45$) but no attempt was made to obtain a full description of how t_s varies with elasticity. For a viscous shear-thinning power-law model Sestak and Charles (1968) first, and Balmer and Fiorina (1980) later, have considered with an approximate asymptotic approach and a finite-difference method, respectively, the start-up problem in a tube, and provide a graphical representation of the variation of t_s with the power-law index. On the other hand, for viscoelastic fluids the only works where a more in depth study of the dependency of t_s on elasticity for the UCM model are those of Ren and Zhu (2004) and Zhen and Zhu (2010), who cite Letelier and Céspedes (1988), with these studies exhibiting an oscillatory variation of t_s versus E . In the present work, a study of the dependence of start-up times on fluid elasticity is carried out for the two rheological models mentioned above. The flow geometry is represented in Fig. 1.

2. Formulation of the problem

The governing equations involve conservation of mass and momentum and a constitutive relationship for the fluid (Oldroyd, 1950; Bird *et al.* 1987). For the solution of those equations it is assumed that the flow is fully developed and no-slip conditions apply at the duct walls.

Conservation of mass in incompressible flow is expressed by the equation:

$$\nabla \cdot \mathbf{u} = 0 \Leftrightarrow \frac{\partial u}{\partial x} + \frac{1}{y^m} \frac{\partial (y^m v)}{\partial y} = 0 \quad (1)$$

where \mathbf{u} represents the velocity vector with Cartesian or cylindrical components u and v relative to the spatial variables x (along duct centreline) and y (representing either a transversal, y , or a radial, r , direction). Index m allows us to deal simultaneously with the two situations: $m=0$ for the planar case; $m=1$ for the axi-symmetric case. Under the

conditions of fully developed flow we have $\partial u / \partial x = 0$ which, together with boundary condition of no slip at the walls ($y=H$, half-width of channel, or $y=R$, pipe radius), allows us to conclude through Eq. (1) that $v=0$.

Conservation of momentum is expressed by:

$$\rho \frac{D\mathbf{u}}{Dt} = -\nabla p + \nabla \cdot \boldsymbol{\tau} \quad (2)$$

where ρ represents the fluid density, p the pressure and $\boldsymbol{\tau}$ the extra stress tensor. For fully developed conditions, Eq. (2) becomes,

$$\rho \frac{\partial u}{\partial t} = -\frac{dp}{dx} + \frac{1}{y^m} \frac{\partial (y^m \tau_{xy})}{\partial y} \quad (3)$$

where τ_{xy} is the shear viscoelastic stress component.

The viscoelastic stress tensor obeys the Oldroyd-B (Oldroyd, 1950) differential constitutive relation:

$$\boldsymbol{\tau} + \lambda \overset{\nabla}{\boldsymbol{\tau}} = 2\eta_0(\mathbf{D} + \lambda_r \overset{\nabla}{\mathbf{D}}) \quad (4)$$

where λ and λ_r are the relaxation and retardation times of the fluid, \mathbf{D} is the rate of deformation tensor and $\overset{\nabla}{\boldsymbol{\tau}}$ the upper convected derivative (Oldroyd, 1950) of the stress tensor, defined as

$$\overset{\nabla}{\boldsymbol{\tau}} = \frac{\partial \boldsymbol{\tau}}{\partial t} + (\mathbf{u} \cdot \nabla) \boldsymbol{\tau} - \boldsymbol{\tau} \cdot \nabla \mathbf{u} - (\nabla \mathbf{u})^T \cdot \boldsymbol{\tau} \quad (5)$$

and similarly for $\overset{\nabla}{\mathbf{D}}$. The relaxation time gives an indication of the magnitude of the elastic nature of the fluid all else being equal. As the relaxation time increases so does the fluid elasticity and a vanishing value corresponds to the Newtonian fluid. It is possible (Bird *et al.* 1987) to decompose the stress tensor of the Oldroyd-B model into Newtonian solvent and “polymeric” elastic components, giving rise to solvent and polymer viscosity parameters η_s and η_p related in the following way

$$\eta_0 = \eta_s + \eta_p, \quad \beta = \frac{\eta_s}{\eta_0} = \frac{\lambda_r}{\lambda} \quad (6)$$

In the case of the upper convected Maxwell (UCM) model $\beta=0$, implying $\eta_s=0$, which entails the absence of explicit diffusion terms in the momentum conservation equation; on the other hand, for the Oldroyd-B we have $\beta \neq 0$ and the model can be seen as a linear combination of UCM and Newtonian models. Under fully developed conditions, Eq. (4) gives $\tau_{yy}=0$ and

$$\tau_{xy} + \lambda \frac{\partial \tau_{xy}}{\partial t} = \eta_0 \left(\frac{\partial u}{\partial y} + \lambda_r \frac{\partial u}{\partial t} \right) \quad (7)$$

for the shear stress component.

Start-up flow is characterised by the sudden imposition, at an initial time instant $t=0$, of a constant pressure gradient that drives the flow, $dp/dx = Cte$. With the simplifying conditions here assumed, Eqs. (3) and (7) may be combined to eliminate the shear stress, yielding the fol-

lowing equation of motion:

$$\left(1 + \lambda \frac{\partial}{\partial t}\right) \frac{\partial u}{\partial t} = -\frac{1}{\rho} \left(1 + \lambda \frac{\partial}{\partial t}\right) \frac{dp}{dx} + \frac{\eta_0}{\rho} \left(1 + \lambda_r \frac{\partial}{\partial t}\right) \left(\frac{1}{y^m} \frac{\partial}{\partial y} \left(y^m \frac{\partial u}{\partial y}\right)\right) \quad (8)$$

whose solution (Waters and King, 1970 and 1971) for either planar channel flow or axi-symmetric pipe flow, in non-dimensional form, can be written as

$$u^*(t^*, y^*) = \kappa(1 - y^{*2}) - \kappa 2^{2+m} \sum_{n=1}^{\infty} \left\{ Z_n^3 F_n(y^*) \left[\exp\left(-\frac{\alpha_n t^*}{2E}\right) G_n(t^*) \right] \right\} \quad (9)$$

on the basis of the following dimensionless variables

$$y^* = \frac{y}{H} \frac{r}{R} \quad t^* = \frac{t}{(\rho H^2 / \eta_0)}, \frac{t}{(\rho R^2 / \eta_0)} \quad u^* = \frac{u}{u_\infty} \quad (10a)$$

where

$$\bar{u}_\infty = \frac{H^2}{3\eta_0} \frac{dp}{dx} \quad (\text{channel}) \quad \text{or} \quad \bar{u}_\infty = \frac{R^2}{8\eta_0} \frac{dp}{dx} \quad (\text{pipe}) \quad (10b)$$

is the average velocity for steady Newtonian channel or pipe Poiseuille flow for a fluid having a total viscosity of η_0 . There is a well-known relation between centreline and average velocities in Poiseuille flow, $u_0 = \kappa \bar{u}_\infty$, with $\kappa = 1.5$ for channel flow and $\kappa = 2$ for pipe flow. The spatial function inside the infinite series of Eq. (9) depends on the geometry; for channel flow, Waters and King (1970) derived:

$$F_n(y^*) = \sin(Z_n(1 + y^*)) \quad \text{with}$$

$$Z_n = (2n - 1)\pi/2 \quad (\text{channel}) \quad (11a)$$

and for pipe flow Waters and King (1971) obtained:

$$F_n(y^*) = \frac{J_0(Z_n y^*)}{J_1(Z_n)} \quad \text{with} \quad Z_n \Leftrightarrow J_0(Z_n) = 0 \quad (\text{pipe}). \quad (11b)$$

Here J_0 and J_1 are Bessel functions of the first kind and for the pipe case Z_n are the zeros of J_0 . The time dependence of the solution has a decaying exponential term and an additional function for the viscoelastic fluids defined by:

$$G_n(t^*) = \cosh\left(\frac{\beta_n t^*}{2E}\right) + \frac{\gamma_n}{\beta_n} \sinh\left(\frac{\beta_n t^*}{2E}\right) \quad (12a)$$

or

$$G_n(t^*) = \cos\left(\frac{\beta_n t^*}{2E}\right) + \frac{\gamma_n}{\beta_n} \sin\left(\frac{\beta_n t^*}{2E}\right) \quad (12b)$$

depending on the sign of $\beta_n^2 = \alpha_n^2 - 4EZ_n^2$: Eq. (12a) if $\beta_n^2 \geq 0$; Eq. (12b) if $\beta_n^2 < 0$. The other parameters are defined below,

$$\alpha_n = 1 + \beta EZ_n^2, \quad \beta_n = \sqrt{\alpha_n^2 - 4EZ_n^2} \quad \text{and}$$

$$\gamma_n = 1 - (2 - \beta)EZ_n^2 \quad (13)$$

As the previous equations show, the analytical solution depends only on two dimensionless groups, the retardation ratio β defined in Eq. (6) and the elasticity number defined by:

$$E = \frac{\lambda \eta_0}{\rho H^2} \quad (\text{channel}) \quad \text{or} \quad E = \frac{\lambda \eta_0}{\rho R^2} \quad (\text{pipe}). \quad (14)$$

To simplify the notation, the asterisk indicating a dimensionless variable will be omitted from now on. It is noted that time is here scaled with a diffusion time scale (see Eq. 10a) and not with the relaxation time of the fluid as is common in situations involving viscoelastic fluid flow. For the Newtonian case the appropriate limit is found by letting $E \rightarrow 0$ and $\beta \rightarrow 1$ or, more directly, the solution is identical to Eq. (9), with $G_n(t) = 1$ and $\alpha_n/E = \pi^2 n^2/2$.

3. Procedure to calculate the start-up time

Taking the limit $t \rightarrow \infty$ in Eq. (9), we see that the transient viscoelastic solution tends to the same steady solution of Newtonian flow, a well-known result. Now, with the aim of estimating the speed with which the solution given by Eq. (9) approaches the Poiseuille solution, depending on the elasticity of the fluid, we need to define and calculate a value of time which we shall designate as the start-up time, t_s . As a first attempt for such a definition we start by considering the difference between the velocity at a particular time instant and the velocity at infinite time (at steady state),

$$d = \|\mathbf{u}(t) - \mathbf{u}_\infty\| \quad (15)$$

where the measure is based on the L_2 norm. To be specific, starting with Eq. (9) we calculate the square of the deviation of the solution in relation to the steady parabolic profile:

$$\sigma^2 = \frac{1}{N_y} \sum_{y_j=1}^{N_y} \left\{ -\frac{48}{\pi^3} \sum_{n=1,3,5}^{\infty} \left[n^{-3} \sin\left(\frac{1}{2}\pi n(1 + y_j)\right) \exp\left(-\frac{\alpha_n t}{2E}\right) G_n(t) \right] \right\}^2 \quad (\text{channel}) \quad (16a)$$

$$\sigma^2 = \frac{1}{N_r} \sum_{r_j=1}^{N_r} \left\{ -16 \sum_{n=1}^{\infty} \left[\frac{J_0(Z_n r)}{Z_n J_1(Z_n)} \exp\left(-\frac{\alpha_n t}{2E}\right) G_n(t) \right] \right\}^2 \quad (\text{pipe}) \quad (16b)$$

for the planar and axi-symmetric cases, respectively. In these equations N_y and N_r are the number of internal points used to resolve the spatial variation of the velocity profile; we have used $N_y = N_r = 50$ but the exact value is irrelevant provided the profiles are adequately represented. Assuming now a tolerance parameter ε (we used $\varepsilon = 0.01$), the start-

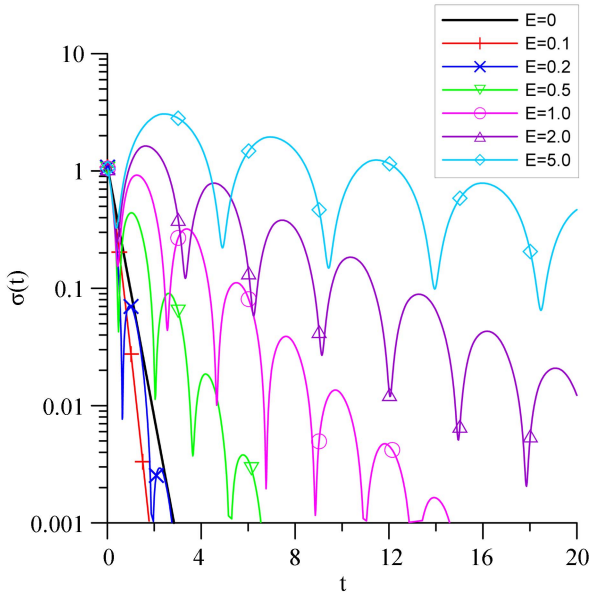


Fig. 2. Evolution of the difference between the solution at time t and at steady state, for various values of the elasticity number (UCM model, channel flow).

up time t_s corresponds to the instant in time after which we have $\sigma < \varepsilon$, that is,

$$t_s = t \text{ such that, for } t > t_s \Rightarrow \sigma < \varepsilon \quad (17)$$

This simple “direct” procedure is adequate for the start-up of Newtonian flow; however, for non-Newtonian fluids oscillations are commonly generated in the initial stages of flow development, as shown in Fig. 2. This figure depicts the evolution for channel flow of the parameter defined by Eq. (16a) for the UCM model and various values of the elasticity number. For $E=0$ (Newtonian fluid) and $E=0.1$, the decay of σ is monotonic, being easy to define a start-up time in accord with inequality (17); however, for $E \geq 0.2$ the evolution of the difference between the solution at time t and the solution at steady state has become oscillatory, making it possible for multiple definitions of such a start-up time.

Other ways of measuring the decay of the solution until it reaches a final steady state lead as well to oscillatory behaviour, with steeper variations than those shown in Fig. 2. In fact, the use of the quadratic mean allows to a certain extent the smoothing out of the temporal evolution of velocities. For example, the centreline velocity for UCM channel flow varies as shown in Fig. 3a, and the departure from its final value $u_{0\infty} = 1.5$ is shown in Fig. 3b. There exists an evident discontinuity in the derivative of $u_0(t) \equiv u(t, y=0)$, which makes it more problematic to use of the centreline velocity for the calculation of start-up times. Physically this discontinuity arises from the formation of a stress wave front at the initial time, which then propagates along the channel for subsequent times, is reflected by the

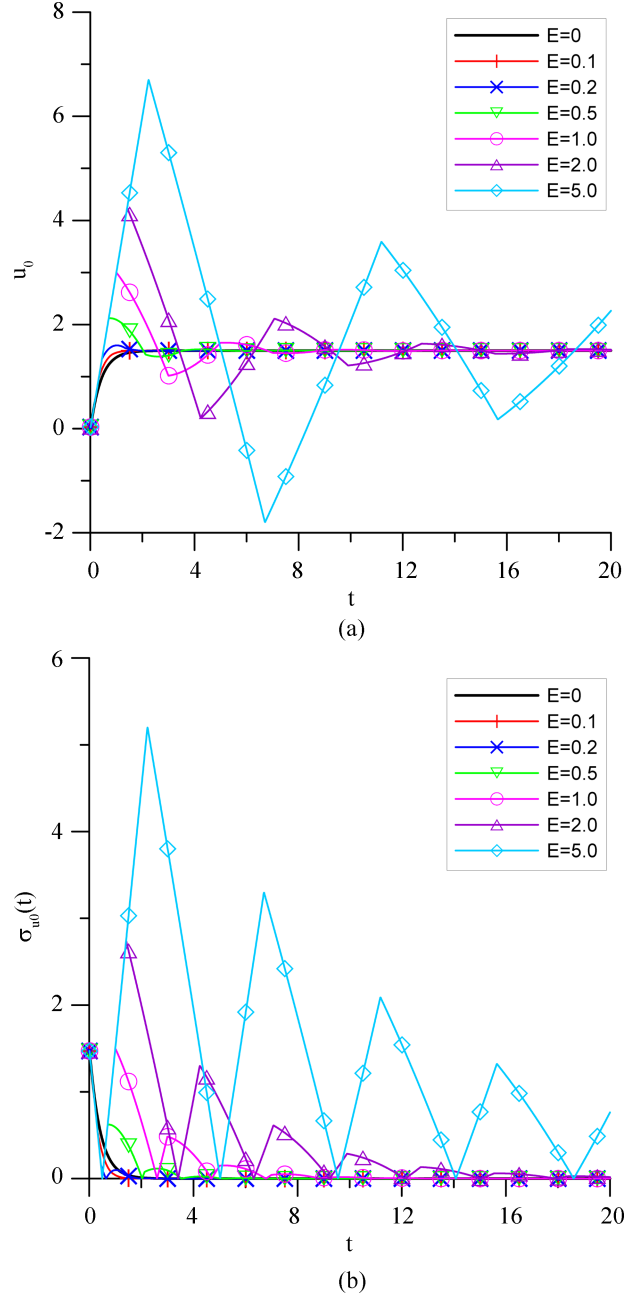


Fig. 3. Time evolution in channel flow of: (a) velocity at centreline, u_0 ; (b) difference between u_0 and its value at steady state (UCM, various elasticity numbers).

walls, and whose magnitude is gradually attenuated but without dissipation (this situation is very clear in Fig. 3 for high values of elasticity; see also Duarte *et al.* 2008).

Fig. 3 is useful as it suggests a different procedure for the calculation of the start-up time. To overcome this problem it suffices to draw an enveloping curve through the points corresponding to the maximum differences between velocity at any instant in time and its value at infinity, and the start-up time will be defined by the condition:

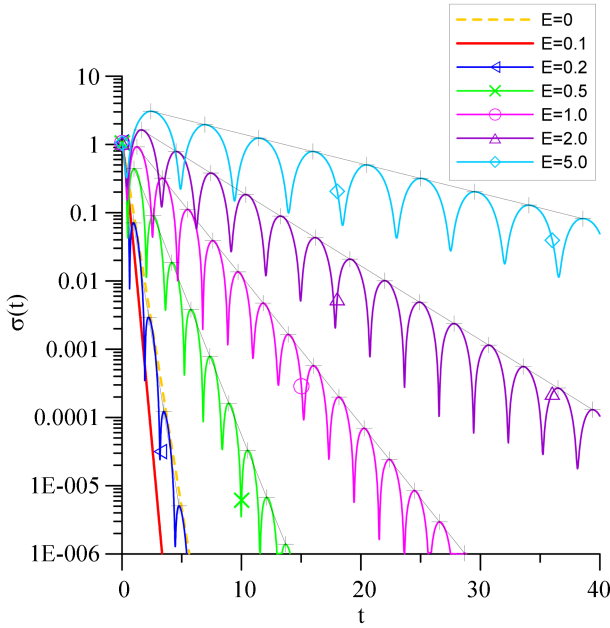


Fig. 4. Exponential-law fittings to the maxima of the variation of $\sigma(t)$ with time, for various elasticity numbers with the UCM model in channel flow.

$$t_s = t \text{ such that } Env[\sigma_{max}(t)] \leq \varepsilon. \quad (18)$$

Although it is not evident in Fig. 3b, it was verified that the decay of the points having maximum σ in a semi-logarithmic scale appear as a straight line, a feature which will help in the interpolations and extrapolations required for determining the start-up times. Fig. 4, showing again some of the data of Fig. 2, illustrates the previous consideration: the cross symbols denote points located at a local maximum of the variation of $\sigma(t)$, each coloured curve corresponds to a given elasticity value E for the UCM model, and the “rectilinear” black lines are curve fittings made automatically by the graphing program according to an exponential function.

From these comments, the proposed procedure for the calculation of the start-up time will take the following steps:

Calculate the points of local maximum of the variation of $\sigma(t)$

in a pre-specified interval $0 \leq t \leq t_{max}$: $\sigma_{max,k} = \max_{|t-t_k| < tol} \{\sigma(t_k)\}$, where t_k ($k=1,2,\dots,N_k$) are time instants for which the N_k maxima do occur.

Adjust a smooth envelope curve to those maxima points, $Y(t)$ such that $Y(t_k) = \sigma_{max,k}$

On a semi-logarithmic scale the variation of the function $Y(t)$ is expected to be close to a straight line defined as:

$$\log Y(t) = At + B \quad (19)$$

The fitting constants in Eq. (19) may be given automatically by the plotting package (using a least squares

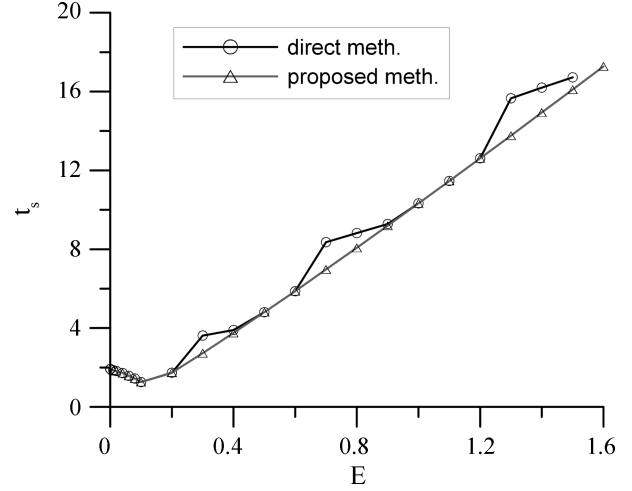


Fig. 5. Effect of method used to calculate start-up times (UCM model, channel flow).

method) or are calculated from two local maxima values (t_1, Y_1) and (t_2, Y_2) :

$$A = (\log Y_2 - \log Y_1) / (t_2 - t_1) \text{ and}$$

$$B = (t_2 \log Y_1 - t_1 \log Y_2) / (t_2 - t_1) \quad (20)$$

Finally, the start-up time is calculated on the basis of statement (18), taking into account the exponential variation of $Y(t)$ from Eq. (19), that is:

$$t_s = (\log(\varepsilon) - B) / A \quad (21)$$

4. Results

We start by showing the discrepancies that arise when the direct method to evaluate the start-up time is used (Eq. 17), instead of the more elaborate procedure just explained (Eqs. 18-21). Fig. 5 shows the variation of t_s in channel flow for the UCM fluid, with the results from the two procedures distinguished as “direct method” and “proposed method”. It is plain that the new procedure produces a smooth variation of the start-up time as a function of the elasticity number, while the direct evaluation of t_s gives rise to unphysical oscillations (wiggles). In previous studies (Ren and Zhu, 2004; Letelier, 1988) this type of oscillations was also apparent. We note that such oscillations are not removed by using a tighter stopping tolerance, such as $\varepsilon = 10^{-4}$ or 10^{-5} , as was demonstrated by the study of Ren and Zhu (2004) for relatively low elasticity numbers ($E \leq 0.16$), and it is also apparent in the oscillating decay of $\sigma(t)$ in Fig. 4. In the present study we have decided to keep $\varepsilon = 10^{-2}$ because we are interested in physical meaningful values for the start-up times and the 1% difference with the steady solution is a commonly used criterion to define t_s (at least for Newtonian flows).

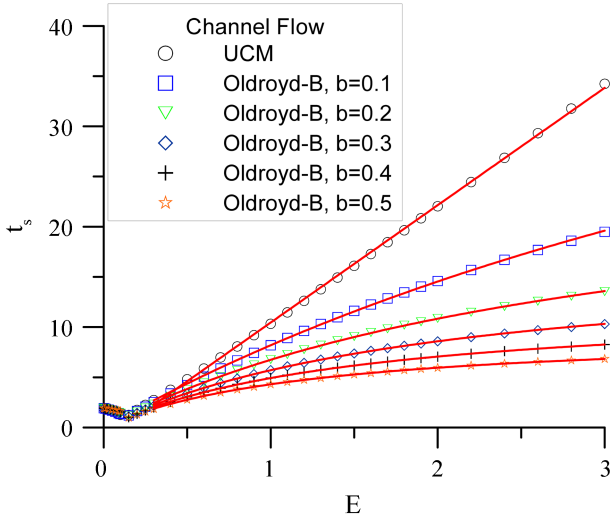


Fig. 6. Variation of start-up time with elasticity in channel flow (UCM and Oldroyd-B models). Lines are curve fittings following Eqs. (22) or (25).

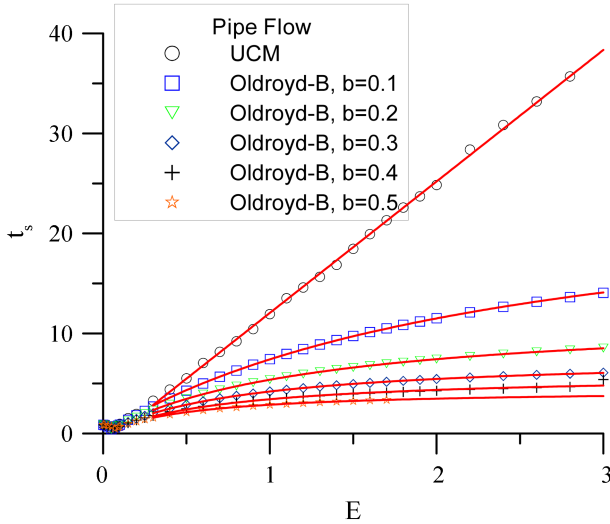


Fig. 7. Variation of start-up time with elasticity in pipe flow (UCM and Oldroyd-B models). Lines are curve fittings following Eqs. (22) or (25).

Our results for the upper convected Maxwell model and the Oldroyd-B model with the retardation ratio, β , varying from 0.1 to 0.5, are shown in Fig. 6 and 7, for channel and pipe flow respectively. In general, there is an initial small decay of the start-up time, from the Newtonian values $(t_s)_N = 1.92$ (channel) and 0.87 (pipe) at $E=0$, up to an elasticity of approximately $E \approx 0.15$ (channel) and 0.05 (pipe), followed by a more marked increase as elasticity is further and progressively incremented. The initial decay of t_s is virtually independent of β , while the later significant increase, as E grows, depends clearly on the value of β . For the UCM fluid the variation is essentially linear; for $E \geq 0.3$, we have a variation well correlated by a straight

Table 1. Coefficients for the linear and fractional curve fittings (Eqs. 22 and 25) of the start-up time.

Channel				Pipe		
β	a	b	c	a	b	c
0	-1.243	11.69	0	-1.095	13.15	0
0.1	0	9.38	1.45	0	10.41	4.05
0.2	0	8.92	1.62	0	9.70	4.03
0.3	0	8.50	1.64	0	9.11	3.91
0.4	0	8.11	1.62	0	8.00	3.34
0.5	0	7.74	1.60	0	8.22	3.72

line:

$$t_s = a + bE \quad (22)$$

with the coefficients a and b provided in Table 1 for both channel and pipe flow. For the Oldroyd-B fluid, the rate of increase of t_s diminishes as β increases and elastic effects tend to die out (we recall that for $\beta=1$ we recover the Newtonian fluid). The variation of t_s versus E is now less than linear (e.g. $t_s = E^{0.8}$ for $\beta=0.1$) and in a first attempt we have applied a polynomial fit of second order, $t_s = a + bE + cE^2$, with the coefficient c being negative; although this fitting gave reasonable correlation of the data, it was not wholly satisfactory because all 3 coefficients varied with β and the functional dependence on this parameter was therefore buried in those coefficients.

A better approach is to design the correlation guided by the form of the analytical solution, Eq. (9). Since the exponential term decays very fast, we can retain only the first term of the series, and for elasticity numbers greater than a critical value the $G_n(t)$ function takes the sinusoidal form of Eq. (12b), which is bounded by one. In this case, the condition that $\mathbf{u} - \mathbf{u}_\infty$ is smaller than ε in Eq. (9) allows us to estimate the start-up time as:

$$t_s = \frac{2E}{1 + Z_1^2 \beta E} \ln \left[\frac{\kappa 2^{2+m} F_1(0)}{\varepsilon Z_1^3} \right] \quad (23)$$

For channel flow ($m=0$) we have $Z_1 = \pi/2$ and $F_1(0)=1$, while for pipe flow ($m=1$) $Z_1=2.4048$ and $F_1(0)=1/J_1(Z_1)$ with $J_1(Z_1)=0.5191$; when these values are substituted in Eq. (23), we obtain the following expected variation of t_s with β and E :

$$t_s = \frac{10.084E}{1 + 2.467\beta E} \text{ (channel) and } t_s = \frac{10.802E}{1 + 5.783\beta E} \text{ (pipe)} \quad (24)$$

We have therefore decided to correlate t_s with the linear fractional function:

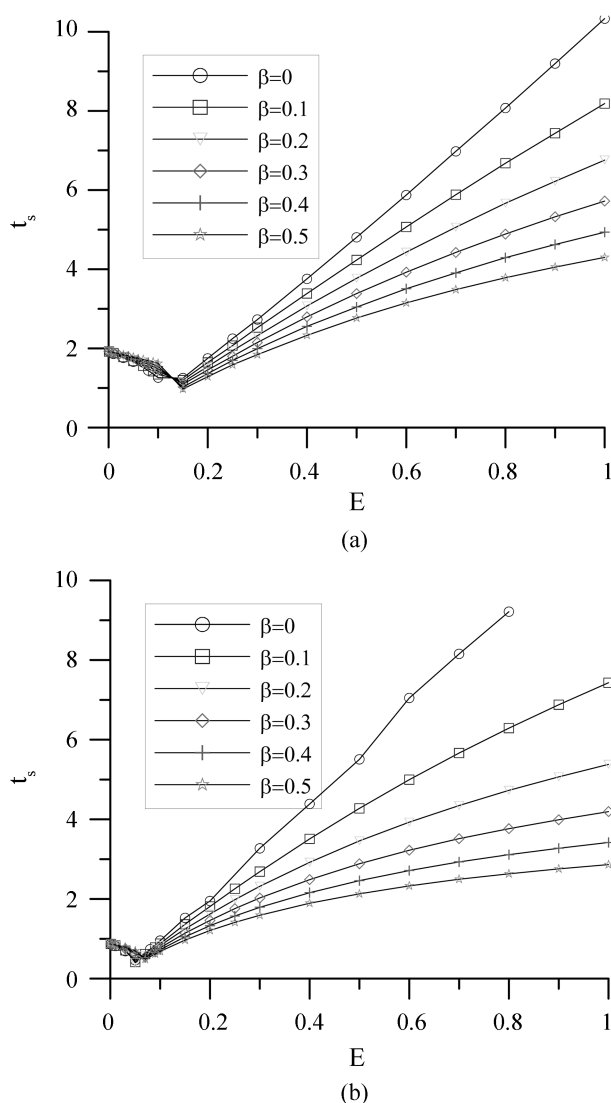


Fig. 8. Detail of the variation of the start-up time in the region $0 \leq E \leq 1$: (a) channel; (b) pipe.

$$t_s = \frac{a + bE}{1 + c\beta E} \quad (25)$$

which gave an extremely good fit, with the a , b and c coefficients contained in Table 1 (valid for $E \geq 0.3$). For $\beta \neq 0$ the a coefficient is unnecessary ($a=0$) but in this way Eq. (25) also contains the linear fit of Eq. (22). The continuous red lines in Fig. 6 and 7 represent the linear and fractional fits defined by Eqs. (22) and (25), which are only applied for elasticity numbers greater than 0.3.

Fig. 8 shows in greater detail the behaviour of the start-up times for relatively low values of elasticity ($E \leq 1$) so that it becomes possible to substantiate the above claim on the independence of t_s relative to β . It is clear from this figure that in the region before the point after which t_s starts growing, there is little sensitivity to variations of the retardation ratio β . For

Table 2. Critical values of elasticity calculated from Eq. (26)

β	E_{cr}	
	channel	pipe
0	0.101	0.0432
0.1	0.107	0.0455
0.2	0.113	0.0482
0.3	0.120	0.0513
0.4	0.129	0.0549
0.5	0.139	0.0593

the Newtonian case the values found are $t_s=1.92$ (channel) and $t_s=0.87$ (pipe), slightly different from the values that result from the theoretical expression (Eq. 9) when only the first term of the infinite series is kept and the departure measured with the centreline velocity: $(48/\pi^3)\exp(-(\pi^2 t_s)/4) = \varepsilon$, $\Rightarrow t_s = 2.04$ (channel), and $((16/J_1(Z_1))/Z_1^3)\exp(-Z_1^2 t_s) = \varepsilon$, $\Rightarrow t_s = 0.93$ (pipe), with the tolerance $\varepsilon=0.01$. This slight difference arises because here we do an integration of the velocity profile along the transversal direction y . We note that these time values differ from those mentioned in the Introduction because velocities are here scaled with their steady-state averaged values and not with centreline values. In Fig. 8 the lines are simple connections between the data points represented by symbols. The minimum values of the calculated start-up time always occurred at $E=0.10-0.15$ (channel) and $E=0.05-0.07$ (pipe), independently of the retardation ratio β . Those minima correlate well with the change of sign of β_n^2 (Eq. 13) when the $G_n(t)$ function becomes trigonometric (Eq. 12b) instead of hyperbolic (Eq. 12a): for $\beta=0$, $\beta_n = 0 \Rightarrow E_{cr} \cong 1/4Z_1^2$; that is, $E_{cr} \cong 1/\pi^2 = 0.101$ for channel flow and $E_{cr} \cong 1/4Z_1^2 = 0.043$ for pipe flow. When $\beta \neq 0$, the theoretically-based critical elasticity number obtained from the zero of β_1 with physical significance is:

$$E_{cr} = \left(\frac{1 - \sqrt{1 - \beta}}{Z_1 \beta} \right)^2 \quad (26)$$

For $E \leq E_{cr}$, t_s decreases with E and there is only a slight dependence on β ; for $E > E_{cr}$, t_s increases with E and depends markedly on β . Values of E_{cr} obtained from Eq. (26) are listed in Table 2 for $\beta=0.0-0.5$ and are indeed seen to be in the range mentioned above, found from the numerical procedure to obtain t_s .

The next two figures for the channel flow case illustrate some detailed aspects of the calculation of the start-up time. The evolution with time of the difference between the velocity profile in channel flow at a certain instant and at steady state, for the UCM case with an elasticity number of 0.5, is shown in Fig. 9. For comparison, the corresponding

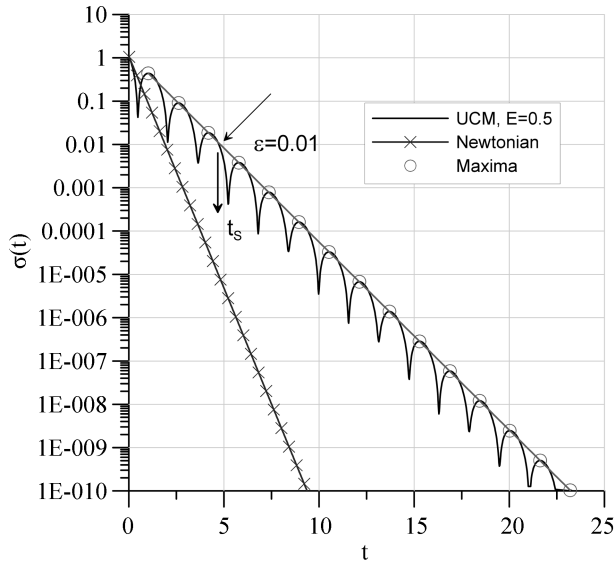


Fig. 9. Evolution with time of the “distance” $\sigma(t)$ for Newtonian and UCM cases with elasticity $E=0.5$.

variation for the Newtonian case is also shown. While in this latter case the decay of the distance is quick and monotonic for the viscoelastic fluid oscillations are present, whose relative magnitudes remain constant with time because the rheological model employed does not possess a “Newtonian” or “solvent” viscosity contribution. Hence, there is no mechanism to dissipate the stress and velocity “shock-waves” propagating across the channel, which are generated by the initial discontinuity of stress at the duct walls. The figure also shows the maxima values as calculated by the computer program, and the “curve” of the exponential-law fitting (a straight line on the semi-log scale employed) which was done automatically by the plotting package. The corresponding function provided by the plotting package is $\ln(Y) = -0.9998 * X + 0.2049$, which allows us to obtain the start-up time ($Y=0.01$) as $X = (\ln(0.01) - 0.2049) / (-0.9998) = 4.811$ (the value obtained from the simulation code, shown in Fig. 6, is $t_s = 4.8045$).

A similar situation, but with the Oldroyd-B model ($\beta = 0.4$) at a point when the oscillatory behaviour is about to be initiated, is shown in Fig. 10. The case with $E=0.15$ corresponds to the point when t_s has just reached its minimum value, and we note that it is then necessary to extrapolate the envelope curve in order to obtain the start-up time. The black line is for the Newtonian fluid, allowing us to verify that for the situation shown the viscoelastic fluids approach the steady state faster (under a normal scale, for example like that of Fig. 4, the decay would be very fast and the oscillations would be unnoticed in a graph). It is interesting to mention here that for $E=0.15$ the start-up time found by the proposed procedure was $t_s = 1.0226$, while the direct method (that is, t for $\sigma(t) \leq \epsilon$) would give $t_s = 1.22$. In a graph of t_s versus E , this difference would be

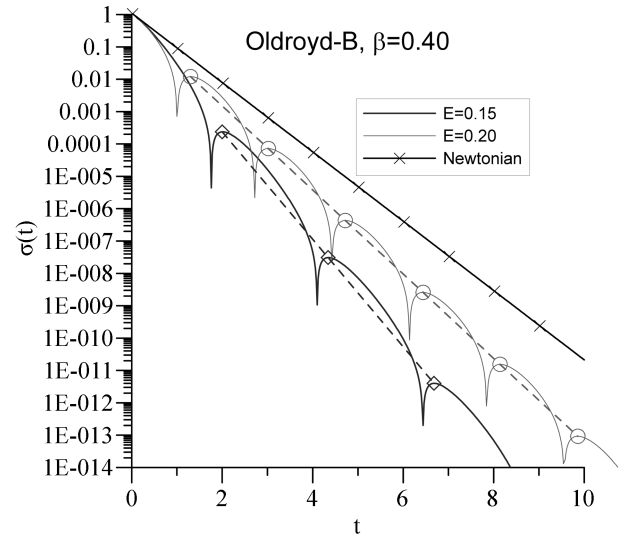


Fig. 10. Evolution of the “distance” $\sigma(t)$ for the Oldroyd-B model with 2 values of elasticity.

sufficiently large to produce a small perturbation similar to the ones observed in Fig. 5.

It is also evident from both Figs. 9 and 10 that a well defined period of oscillation exists once the evolution of the flow to steady state becomes sinusoidal. That period may be approximated by the first term of the infinite series, $G_1(t)$ in Eq. (12b), yielding:

$$T = 2\pi \frac{2E}{\beta_1} = 2\pi \frac{\sqrt{E}}{Z_1 \sqrt{1 - \left(\frac{1 + Z_1^2 \beta E}{2Z_1 \sqrt{E}} \right)^2}} \quad (27)$$

When $\beta = 0$ for the UCM model, this expression shows that the half period increases as $T/2 = \frac{\pi}{Z_1} \sqrt{E} (1 + 1/8 Z_1^2 E)$, or $T \approx \sqrt{E}$ for $E \geq 1$; for the Oldroyd-B, even at high E , it is not easy to further simplify Eq. (27). For the cases in Figs. 9 and 10, Eq. (27) gives half-periods of $T/2 = 1.58$ (UCM, $E=0.5$), 2.34 ($\beta=0.4$, $E=0.15$) and 1.71 ($\beta=0.4$, $E=0.2$), in close agreement with the values measured from the figures, by taking the time gap between two consecutive peaks in the graphs.

5. Conclusions

A simple procedure to calculate start-up times in channel and pipe flows of viscoelastic fluids was devised and implemented in a simulation code. The results obtained show a significant increase of the start-up times, of about 18 (channel) or 41 (pipe) fold when elasticity goes from 0 (Newtonian case) up to $E=3$, with the UCM model. This increment of the time required for the flow to be established tends to decrease as the fluid elasticity decreases, either by a reduction of E or by an increase of β . When the elasticity

of the fluid is only marginally greater than zero, for liquids with low elasticity ($E \leq E_{cr}$, with $E_{cr} \approx 0.10-0.15$, channel, and $E_{cr} \approx 0.05-0.07$, pipe) the flow development is quicker than for Newtonian fluids, and the start-up time becomes almost independent of the relative value for the solvent viscosity (that is, of the model parameter β). In practical terms this study provides a useful correlation for the calculation of start-up times as a function of E and β , the fractional function of Eq. (25) which reduces to a linear variation when $\beta = 0$ (UCM model). This correlation is valid when E is greater than a critical value E_{cr} defined by Eq. (26), separating the region of decreasing and increasing start-up times with elasticity. In the oscillatory regime, the period of oscillation was found to be approximated by Eq. (27). As an illustrative example, if we consider blood flow in an artery with 2 mm diameter, assuming blood to be viscoelastic with a relaxation time of $\lambda = 0.145$ s, viscosity of $\eta_0 = 5 \times 10^{-3}$ Pa.s and plasma viscosity of $\eta_s = 10^{-3}$ Pa.s, then we have an elasticity number of $E = 0.63$ and correlation Eq. (25) gives $t_s = 4.0$ (with the parameters of Table 1 for pipe flow). Dimensionally, this start-up time is 0.9 s which is of the order of the heart pulse.

Acknowledgments

Financial support by Fundação para a Ciência e a Tecnologia (FCT, Portugal) under project PTDC/EME-MFE/70186/2006 is here gratefully acknowledged. PJO wishes also to thank Universidade da Beira Interior for a sabbatical leave. Special thanks to Dr. R.J. Poole (University of Liverpool) for assistance in proof-reading of the paper.

References

- Akyildiz, F.T. and R.S. Jones, 1993, The generation of steady flow in a rectangular duct, *Rheologica Acta* **32**, 499-504.
- Bird, R.B., R.C. Armstrong and O. Hassager, 1987, *Dynamics of Polymeric Liquids, Vol. 1: Fluid Mechanics*, 2nd ed., John Wiley, New York.
- Balmer, R.T. and M.A. Fiorina, 1980, Unsteady flow of an inelastic power-law fluid in a circular tube, *J. Non-Newtonian Fluid Mech.* **7**, 189-198.
- Bromwich, T.J., 1930, An application of Heaviside's methods of viscous fluid motion, *J. London Math. Soc.* **5**, 10-13.
- Duarte, A.S.R., A.I.P. Miranda and P.J. Oliveira, 2008, Numerical and analytical modeling of unsteady viscoelastic flows: the start-up and pulsating test case problems, *J. Non-Newtonian Fluid Mech.* **154**, 153-169.
- Letelier, M.F. and J.F. Céspedes 1988, *Laminar Unsteady Flow of Elementary Non-Newtonian Fluids in Long Pipes*, Chapter 3 in *Encyclopedia of Fluid Mechanics*, Vol. 7, *Rheology and Non-Newtonian Flows*, Ed. N.P. Cheremisinoff, Gulf Publishing Company, Houston, 55-87.
- Oldroyd, J.G., 1950, On the formulation of rheological equations of state, *Proc. R. Soc. A* **200**, 523-541.
- Park, K.S. and Y.D. Kwon, 2009, Numerical description of start-up viscoelastic plane Poiseuille flow, *Korea-Australia Rheology J.* **21**, 47-58.
- Rahaman, K.D. and H. Ramkissoon, 1995, Unsteady axial viscoelastic pipe flows, *J. Non-Newtonian Fluid Mech.* **57**, 27-38.
- Ren, L. and K-Q. Zhu, 2004, Dual role of viscosity during start-up of a Maxwell fluid in a pipe, *Chin. Phys. Lett.* **21**, 114-116.
- Sestak, J. and M.E. Charles, 1968, An approximate solution for start-up flow of a power-law fluid in a tube, *Chem. Eng. Sci.*, **23**, 1127-1137.
- Szymanski, P., 1932, Quelques solutions exactes des equations de l'hydrodynamique du fluide visqueux dans le cas d'un tube cylindrique, *J. Math. Pures Appl. (Series 9)* **11**, 67-107.
- Waters, N.D. and M.J. King, 1970, Unsteady flow of an elastico-viscous liquid, *Rheologica Acta* **9**, 345-355.
- Waters, N.D. and M.J. King, 1971, The unsteady flow of an elastico-viscous liquid in a straight pipe of circular cross section, *J. Phys.D: Appl. Phys.* **4**, 204-211.
- Wood, W.P., 2001, Transient viscoelastic helical flows in pipes of circular and annular cross-section, *J. Non-Newtonian Fluid Mech.* **100**, 115-126.
- Zhen, L. and K-Q. Zhu, 2010, Effects of relaxation time on start-up time for starting flow of Maxwell fluid in a pipe, *Acta Mech. Sin.* **26**, (in press).